



A nonstructural 2B protein of enterovirus A71 increases cytosolic Ca^{2+} and induces apoptosis in human neuroblastoma SH-SY5Y cells

Oratai Supasorn¹ · Pongsri Tongtawe¹ · Potjane Srimanote¹ · Patthaya Rattanakomol¹ · Jeeraphong Thanongsaksrikul¹

Received: 24 August 2019 / Revised: 22 November 2019 / Accepted: 16 December 2019 / Published online: 13 January 2020
© Journal of NeuroVirology, Inc. 2020

Abstract

Enterovirus A71 (EV-A71) is one of the causative agents causing the hand-foot-mouth disease which associated with fatal neurological complications. Several sporadic outbreaks of EV-A71 infections have been recently reported from Asia-Pacific regions and potentially established endemicity in the area. Currently, there is no effective vaccine or antiviral drug for EV-A71 available. This may be attributable to the limited information about its pathogenesis. In this study, the recombinant nonstructural 2B protein of EV-A71 was successfully produced in human neuroblastoma SH-SY5Y cells and evaluated for its effects on induction of the cell apoptosis and the pathway involved. The EV-A71 2B-transfected SH-SY5Y cells showed significantly higher difference in the cell growth inhibition than the mock and the irrelevant protein controls. The transfected SH-SY5Y cells underwent apoptosis and showed the significant upregulation of caspase-9 (*CASP9*) and caspase-12 (*CASP12*) genes at 3- and 24-h post-transfection, respectively. Interestingly, the level of cytosolic Ca^{2+} was significantly elevated in the transfected SH-SY5Y cells at 6- and 12-h post-transfection. The caspase-9 is activated by mitochondrial signaling pathway while the caspase-12 is activated by ER signaling pathway. The results suggested that EV-A71 2B protein triggered transient increase of the cytosolic Ca^{2+} level and associated with ER-mitochondrial interactions that drive the caspase-dependent apoptosis pathways. The detailed mechanisms warrant further studies for understanding the implication of EV-A71 infection in neuropathogenesis. The gained knowledge is essential for the development of the effective therapeutics and antiviral drugs.

Keywords Nonstructural 2B protein · Enterovirus A71 · Human neuroblastoma cell · Apoptosis · Calcium signaling pathway

Introduction

Enterovirus A71 (EV-A71) is a nonenveloped, positive-sense, single-stranded RNA virus classified in *Enterovirus A* genus, *Picornaviridae* family. It is a neurotropic virus causing the hand-foot-mouth disease which associated with fatal neurological complications among children less than 5 years old (Chang et al. 1998; Huang et al. 1999; Wu et al. 2002). The complications include aseptic meningitis, brainstem encephalitis, flaccid paralysis, and neurogenic cardiopulmonary failure. Pieces of evidence have demonstrated that tonsillar crypt

epithelium and Peyer's patches are the primary replication sites for EV-A71 (He et al. 2014; Solomon et al. 2010; Xie et al. 2016). In the animal model, EV-A71 virions could get entry into the bloodstream and disseminate to various organs including the central nervous system (CNS) by undefined mechanism (Chen et al. 2007; Ong et al. 2008). The neuropathogenesis of EV-A71 infection has been associated with CNS damage via inflammation and induction of aberrant cell death (Fujii et al. 2013; Lin et al. 2003; Yu et al. 2014). It could be proposed that the virus induces aberrant apoptosis in a nonrenewable neuron which is irreplaceable and results in a premature loss of cells leading to neuropathology.

It has been clearly demonstrated in vitro that EV-A71 could infect both neuronal and non-neuronal cells and induce apoptotic cell death (Chang et al. 2004; Kuo et al. 2002; Li et al. 2002). EV-A71 induced apoptosis in the infected HeLa cells through calpain (encoded by *CAPN2* gene) activation leading to apoptosis inducer factor (AIF)-mediated, caspase-independent apoptosis (Lu

✉ Jeeraphong Thanongsaksrikul
jeeraphong.t@allied.tu.ac.th

¹ Graduate Program in Biomedical Sciences, Faculty of Allied Health Sciences, Thammasat University, 99 Moo 18 Paholyothin Road, Klong Luang, Rangsit, Pathum Thani 12120, Thailand

et al. 2013). EV-A71 induced apoptosis in U251 human astrocyte cell lines by an intrinsic pathway (Wang et al. 2015). Interestingly, motor neuron-like NSC-34 cell line infected with EV71 underwent autophagy instead of apoptosis (Too et al. 2016). Further, EV-A71-infected SH-SY5Y neuroblastoma cells underwent apoptosis by caspase-dependent manners (Du et al. 2015). Hence, apoptosis induced by EV-A71 infection is likely the cell type-specific manner.

Nonstructural 2B proteins are a member of the viroporin family. The enteroviral viroporins are small (97–99 amino acids) transmembrane protein that forms homomultimers on plasma and organelle membranes including ER, Golgi complex, and mitochondria to exert Ca^{2+} conductance channel activity (Ao et al. 2014). They contain two hydrophobic regions, namely, HR1 and HR2 spaced by a short hydrophilic sequence called spacer (Martínez-Gil et al. 2011; van Kuppeveld et al. 1996). The HR1 has been predicted to form an amphipathic α -helix while HR2 formed a completely hydrophobic. The nonstructural 2B proteins of poliovirus 1 (PV-1) and coxsackievirus B3 (CVB-3), the closely related enteroviruses to EV-A71, have been found to alter the intracellular Ca^{2+} homeostasis and modulate cell apoptosis. The PV-1 and CVB-3 2B proteins expressed in the buffalo green monkey (BGM) cells could form transmembrane pore on ER and Golgi complex membrane and exert viroporin activity by causing efflux of Ca^{2+} from the organelles (de Jong et al. 2008). In HeLa cells, PV-1 2B precursor (2BC) facilitated the release of ER-stored Ca^{2+} to the cytoplasm but the determination of apoptosis induction was not performed (Aldabe et al. 1997). While the expression of CVB-3 2B expressed in HeLa cells mediated the release of Ca^{2+} from the ER and Golgi complex into cytoplasm and depleted Ca^{2+} content in these storage sites whereby Ca^{2+} signaling crosstalk between the ER-Golgi complex and the mitochondria were then down-regulated leading to suppression of apoptosis (Campanella et al. 2004). The EV-A71 2B protein was found to localize on the mitochondrial membrane of the HeLa cells and directly modulated redistribution and activation of the pro-apoptotic protein Bax leading to cell apoptosis through the mitochondrial pathway (Cong et al. 2016). However, the mechanism of EV-A71 2B inducing apoptosis in neuronal cells is poorly understood. In this study, we investigated the apoptosis-inducing activity of EV-A71 nonstructural 2B protein in the human neuroblastoma SH-SY5Y cells and elucidated the involved mechanisms. The gained knowledge would not only pave the way for understanding the apoptosis-related neuropathogenesis but eventually be beneficial for the development of a new strategy for the treatment of neurological complications caused by EV-A71 infection.

Materials and methods

Cell lines and virus

Human embryonic kidney 293T cells (Lenti-X™ HEK 293T) and human rhabdomyosarcoma (RD) cells (JCRB9072) were purchased from Clontech (CA, USA) and Japanese Collection of Research Bioresources Cell Bank, respectively. Human neuroblastoma SH-SY5Y cells (ATCC®, CRL-2266™) were a generous gift from Associate Professor Dr. Chintana Chirathaworn, Faculty of Medicine, Chulalongkorn University, Thailand. HEK 293T and RD cells were grown in Dulbecco's modified Eagle's medium (DMEM, Biochrom, Cambridge, UK) and SH-SY5Y cells were cultured in DMEM/F12 (Gibco, NY, USA). Both media were supplemented with 10% fetal bovine serum, L-glutamine, and penicillin/streptomycin antibiotics (Gibco, NY, USA). The cells were incubated at 37 °C in the humidified air containing 5% CO_2 . Enterovirus A71 (EV-A71) subgenotype B5 were propagated in RD cells. The virus titer was determined as described previously (Thanongsaksrikul et al. 2018).

Construction of recombinant plasmid

The coding sequence of EV-A71 nonstructural 2B protein (2B) flanked by coding sequences of FLAG-epitope tag and mCherry fluorescent protein at 5' and 3' end, respectively, was amplified by the overlap extension PCR. Briefly, the 2B coding sequence was amplified from cDNA reverse transcribed from the RNA of EV-A71 subgenotype B5. Sequences of the primers are 5'-**GAATTC**ATGGATTACAAGGATGACGATGACAAGGGTGTCTCTGACTACATTA-3' (Outer1-MamNS2B-Forward); the italic and bold letters are *EcoRI* restriction site, the underlined letters are FLAG-tag coding sequence, and 5'-TCCTCGCCCTTGCTCACCATCTTCTGGCAATGGG-3' (Inner1-2B-mCherry Reverse); the underlined letters are the first 20 nucleotides of *mCherry* coding sequence. The coding sequence of mCherry was amplified from cDNA inserted in pLV-mCherry, a gift from Pantelis Tsoulfas (Addgene plasmid # 36084; <http://n2t.net/addgene:36084>; RRID: Addgene_36,084). Sequences of the primers are 5'-GCATCCCCATTGCCAAGAAGATGGTGAGCAAGGGCGAGGAGGATAACATG-3' (Inner2-2B-mCherry-Forward); underlined letters are the last 20 nucleotides of 2B coding sequence, and 5'-**TCTAGATTAC**TTGTACAGCTCGTCCAT-3' (Outer2-mCherry-Reverse); the italic and bold letters are *XbaI* restriction site. PCRs were performed with *ProFi Taq* DNA polymerase (Bioneer, Daejeon, Republic of Korea). The thermocycling program was 95 °C for 5 min followed by 30 cycles of 95 °C for 30 s, 66 °C for 30 s, and 72 °C for 1 min, finally 72 °C for 3 min. The PCR amplicons of 2B and *mCherry* fragments were resolved by 1% (W/V) agarose gel electrophoresis and

purified from the gel slabs by AccuPrep® gel extraction kit (Bioneer, Daejeon, Republic of Korea). The purified DNA fragments were mixed in PCR mixture without the primers and slowly annealed together at the overlapping-point by initial heating at 95 °C for 5 min followed by lowering the temperature down from 95 to 45 °C with temperature decrement at -2.0 °C/min for 5 min. Their overhang termini were then extended by filling with deoxynucleotides with the extension step at 72 °C for 2 min. Consequently, the full-length DNA template of *FLAG-2B-mCherry* coding sequences was generated. Immediately, the Outer1-MamNS2B-Forward and Outer2-mCherry-Reverse primers were added into the reaction tube and the complete *FLAG-2B-mCherry* coding sequences were amplified by the thermocycling program of 35 cycles of 95 °C for 1 min, 45 °C for 5 min, and 72 °C for 2 min, and final extension step at 72 °C for 4 min. The *FLAG-2B-mCherry* coding sequences were ligated into pGEM® T Easy cloning vector (Promega, Madison, USA) and subcloned into the mammalian protein expression vector pLVX-Puro (Clontech) using *EcoRI* and *XbaI* restriction sites.

Sequence analysis and domain prediction of 2B protein

The coding sequence of *FLAG-2B-mCherry* inserted in pLVX-Puro (designated as pLVX-puro::*FLAG-2B-mCherry*) was verified by DNA sequencing. The DNA sequencing data were analyzed by Applied Biosystem Sequence Scanner Software v1.0 (ABI). The sequence of the cloned 2B was compared with the other EV-A71 and enteroviral 2B sequences in databases using BLAST search (<https://blast.ncbi.nlm.nih.gov/Blast.cgi>). Transmembrane domains of the cloned 2B sequence of EV-A71 and well-annotated sequences of poliovirus 1; PV-1 (de Jong et al. 2008), and coxsackievirus B3; CVB-3 (de Jong et al. 2008), were predicted using Web-Based Hydrophathy and Amphipathicity predictions (WHAT 2.0) (<http://www.tcdb.org/progs/?tool=hydro>), HMMTOP (<http://www.enzim.hu/hmmtop/html/submit.html>), Split 4.0 (<http://splitbioinf.pmfst.hr/split/4/>), and RHYTHM (<http://proteinformatics.charite.de/rhythm/index.php?site=helix>). Multiple alignments of amino acid sequences were performed using Clustal Omega (<https://www.ebi.ac.uk/Tools/msa/clustalo/>). The amphipathic α -helix wheel was predicted using the Helical Wheel Projections (<http://rzlab.ucr.edu/scripts/wheel/wheel.cgi>).

Transient transfection

HEK 293T cells were seeded at a density of 5×10^4 cells/well in a 24-well culture plate. SH-SY5Y cells were seeded at a density of 5×10^5 cells/well in a 6-well, 1×10^5 cells/well in a 24-well, and 3×10^4 cells/well in a 96-well culture plates. The cells were grown until reached approximately 60% confluence

and transfected with pLVX-puro::*FLAG-2B-mCherry* or controls by Lipofectamine™ 3000 reagents according to manufacturer's instructions (ThermoFisher Scientific, CA, USA).

Fluorescent assay, Western blotting, and flow cytometry of FLAG-2B-mCherry protein

Expression of the FLAG-2B-mCherry fusion proteins was detected in cells transfected with pLVX-puro::*FLAG-2B-mCherry* at 24 h post-transfection (h.p.t.) by fluorescent assay, Western blotting and flow cytometry. Cell monolayers transfected with the pLVX-Puro empty vector served as a mock control. The untransfected- and pLV-mCherry-transfected cells served as negative and positive protein expression controls, respectively. For the fluorescent assay, monolayers of the transfected cells grown on a glass slide placed in a 24-well culture plate were fixed with 4% paraformaldehyde for 20 min at room temperature and washed twice with phosphate-buffered saline (PBS). The cell monolayers were mounted with PBS and observed for bright red fluorescence signal of mCherry protein under up-light fluorescent microscope Olympus BX53 (Olympus, Hamburg, Germany). The excitation and emission maximum wavelengths of mCherry fluorescence protein were 587 nm and 610 nm, respectively. For Western blotting, monolayers of transfected cells or controls grown in the 6-well culture plate were washed once with PBS and added with 1-ml ice-cold lysis buffer (100 mM Na-HEPES, pH 7.5, 300 mM NaCl, 2 mM EDTA, 0.5% Triton X-100, 10% glycerol, and protease inhibitor cocktail). The cells were dissociated by repeat pipetting and then homogenized by ultrasonication at 30 amplitudes with a pulse on and off at 5 s for 3 min (SONICS Vibra cell™, Sonics and Material, CT, USA). The cell lysates were collected by centrifugation at 13,000 rpm for 20 min at 4 °C. The proteins in the cell homogenate and lysate fractions were separated by sodium dodecyl sulfate-polyacrylamide gel electrophoresis (SDS-PAGE) and transferred to the nitrocellulose membranes. The blotted membranes were immersed in 5% fetal bovine serum in PBS to block unoccupied areas for 1 h. The membranes were washed with PBS containing 0.05% Tween-20 (PBS-T), incubated with primary antibody; either monoclonal anti-FLAG®M2 (Sigma-Aldrich, MO, USA) or polyclonal anti-mCherry (Biovision, CA, USA) mouse antibodies, and incubated with polyclonal anti-mouse IgG goat antibody conjugated with alkaline phosphatase. Reactive bands of the protein-antibody complex were visualized by NBT/BCIP substrate solution (KPL, SeraCare, MA, USA). For flow cytometry, monolayers of transfected cells or controls grown in the 6-well culture plate were trypsinized and resuspended in a binding buffer from FITC Annexin V apoptosis detection kit I (BD Biosciences, CA, USA). The expression of the mCherry fluorescent protein was determined by BD FACSVerse™ flow cytometer (BD Biosciences, CA,

USA) at maximum excitation and emission at 587 nm and 610 nm, respectively.

Sulforhodamine B assay

Viability and proliferation of the SH-SY5Y cell monolayers transfected with pLVX-puro::FLAG-2B-mCherry or controls were measured by sulforhodamine B (SRB) assay (Orellana and Kasinski 2016; Vichai and Kirtikara 2006). The SH-SY5Y cell monolayers in a 96-well plate were transfected with pLVX-puro::FLAG-2B-mCherry and incubated for 24 h. The cell monolayers dropped with only the transfection reagent served as a mock control. The pLVX::FLAG-3A-mCherry- and pLV::mCherry-transfected cells served as irrelevant controls. The pLVX::FLAG-3A-mCherry encoded the nonstructural 3A protein of EV-A71 fused with FLAG-tag and mCherry at C- and N-terminal ends, respectively (unpublished data). SH-SY5Y cells infected with EV-A71 at 0.1 and 1 multiplicity of infection (M.O.I.) served as cell death control. The cell monolayers were fixed by directly adding 25 μ l of iced-cold 50% (w/v) trichloroacetic acid (Sigma-Aldrich, MO, USA) into each well. The cell monolayers were washed with distilled water and air-dried at an ambient temperature. All wells were added with 50 μ l of 0.04% (w/v) SRB solution (Sigma-Aldrich, MO, USA) and kept at an ambient temperature for 1 h. After that, the wells were rinsed by 1% (v/v) acetic acid to remove the unbound dyes and air-dried. The cell-bound SRB dyes were eluted out by adding 100 μ l of 10 mM Tris base solution pH 10.5 to each well. The optical density (OD) was measured by absorbance at OD_{510nm} by the FlashScan™ microplate reader (Thermo Fisher Scientific, Vantaa, Finland). The percentages of cell growth and cell growth inhibition were calculated by using the formula: % cell growth = (OD_{510nm} of test or irrelevant control \div OD_{510nm} of

mock control) \times 100. Percentages of the cell growth inhibition were calculated by 100 – % cell growth.

Annexin V binding assay

Induction of apoptosis was determined by FITC annexin V apoptosis detection kit I (BD biosciences, CA, USA) according to manufacturer's instructions.

qRT-PCR of apoptosis-related genes

RNA was extracted from the SH-SY5Y cells transfected with pLVX-puro::FLAG-2B-mCherry and infected with 0.1 M.O.I. of the EV-A71 which collected at 1-, 3-, 6-, 12- and 24 h p.t. Control groups were pLV::mCherry-transfected cells, mock transfection, and uninfected cells. The DNaseI-treated RNA samples were used as the templates to amplify the selected apoptosis-related genes including caspase-3 (*CASP3*), caspase-8 (*CASP8*), caspase-9 (*CASP9*), caspase-12 (*CASP12*), apoptosis inducer factor M1 (*AIFM1*), calpain (*CAPN2*), and Bax (*BAX*) by one-step qRT-PCR using Brilliant II SYBR® Green qRT-PCR one-step kit (Stratagene, CA, USA). The gene-specific primers are listed in Table 1. The conditions applied for one-step qRT-PCR were reverse transcription at 42 °C for 60 min, followed by real-time PCR with the initial denaturation at 95 °C for 5 min, 40 cycles of 95 °C for 1 min, 50 °C (for *CASP12*), 55 °C (for *AIFM1* and *CASP8*), or 62 °C (for *CASP3*, *CASP9*, *BAX*, and *CAPN2*) for 1 min, and 72 °C for 45 s, and melting curve analysis. The expression levels of the apoptosis genes were quantified using the $\Delta\Delta$ CT method to determine fold-change ($2^{-\Delta\Delta CT}$) in the gene expression (Rao et al. 2013). Changes in the mRNA expression level were calculated after normalization to the internal control, human β -actin house-keeping gene. The Δ CT of pLVX-

Table 1 Lists of the primers for qRT-PCR of the selected apoptosis-related genes

Name of gene	Sequence of primer	Reference
Human caspase-3 (<i>CASP3</i>)	Forward 5'-CAGTGGAGGCCGACTTCTTG-3' Reverse 5'-TGGCACAAGCGACTGGAT-3'	Srisuwan et al. 2014
Human caspase-8 (<i>CASP8</i>)	Forward 5'-CAGCATTAGGGACAGGAATG-3' Reverse 5'-CAGTTATTCACAGTGGCCAT-3'	In this study
Human caspase-9 (<i>CASP9</i>)	Forward 5'-GTGGACATTGGTTCTGGAGGAT-3' Reverse 5'-CGCAACTTCTCACAGTCGATG-3'	Huang et al. 2017
Human caspase-12 (<i>CASP12</i>)	Forward 5'-GTTCAACATTCATTTGAGACC-3' Reverse 5'-CCTGAGTTGCTTCTTATGAG-3'	In this study
Human Bax (<i>BAX</i>)	Forward 5'-TGGAGCTGCAGAGGATGATTG-3' Reverse 5'-GAAGTTGCCGTGAGAAAACATG-3'	Srisuwan et al. 2014
Human AIFM1 (<i>AIFM1</i>)	Forward 5'-AACTGCACAAGACAACCCCA-3' Reverse 5'-TGACACCTTTGCCGTAGTCC-3'	In this study
Human CAPN2 (<i>CAPN2</i>)	Forward 5'-GCCTTTGAGCTGCAGACCAT-3' Reverse 5'-TGCCTTCCGATTTTCATAGG-3'	In this study
Human β -actin	Forward 5'-GAGCGGGAAATCGTGCATGACATT-3' Reverse 5'-GAAGGTAGTTTCGTGGATGCC-3'	In this study

puro::*FLAG-2B-mCherry*- and pLV::*mCherry*-transfected SH-SY5Y cells were subtracted with those of the mock controls. The fold-changes of the gene expression were derived from the subtractive Δ CT of pLVX-puro::*FLAG-2B-mCherry*-transfected cells relative to those of pLV::*mCherry*-transfected cells. The fold-changes in the gene expression of the infected cells were relative to the uninfected cells.

Cytosolic Ca²⁺ measurement

Cytoplasmic Ca²⁺ in the EV-A71 2B-transfected SH-SY5Y cells was measured by Molecular probes™ Fluo-4 AM, the cell-permeant calcium indicator (Invitrogen, UK). A free-form of the Fluo-4 AM is almost nonfluorescent and its fluorescence increases upon binding with Ca²⁺. Mock and irrelevant controls were cell monolayers dropped with only the transfection reagent and transfected with pLV::*mCherry*, respectively. The 2B transfected- and control cells were collected at 1-, 3-, 6-, 12-, and 24 h p.t. The cell monolayers were trypsinized, washed twice by 1 ml of Hank Balanced Salt Solution (HBSS) (Gibco®, Life Technologies, NY, USA), and centrifuged at 1000 rpm for 5 min. The cells were resuspended in HBSS buffer containing 2 μM Fluo-4 AM. An aliquot of each cell suspensions without Fluo-4 AM served as the unstained control for subtracting the internal background signals. The samples and the controls were measured for the fluorescent signal of Ca²⁺-bound Fluo-4 AM; designated as $F_{\text{test/control}}$, with excitation wavelength at 488 nm and emission wavelength at 535 nm by a FlashScan™ microplate reader. The maximum fluorescent signals; designated F_{max} , was measured from the SH-SY5Y cells pre-incubated with the culture medium containing 2 mM CaCl₂ at 37 °C for 1 h and then added with Fluo-4 AM. After that, the cells were treated with 0.1% Triton-X 100 for 10 min at an ambient temperature and the F_{max} was measured. For minimum fluorescent signals; designated F_{min} , the SH-SY5Y cells were incubated with Fluo-4 AM as described above. Then, the cells were added with 0.1% (v/v) permeabilizing reagent Triton-X 100, incubated for 10 min at an ambient temperature, and added with 20 mM ethylene glycol-bis (β-aminoethyl ether)-N,N,N',N'-tetraacetic acid or EGTA (Sigma-Aldrich, MO, USA). The F_{min} was measured. The $F_{\text{test/control}}$ subtracted with the internal background signals were converted into the cytoplasmic Ca²⁺ ion concentration; $[\text{Ca}^{2+}_{\text{cyto}}]$, by the equation: $[\text{Ca}^{2+}_{\text{cyto}}] = \text{Kd} \times [(F_{\text{test/control}} - F_{\text{min}}) \div (F_{\text{max}} - F_{\text{test/control}})]$. The dissociation constant (Kd) value of Fluo-4 AM to Ca²⁺ was 345 nM (Lock et al. 2015).

Confocal imaging

Localization of apoptosis marker; phosphatidylserine, and cytoplasmic Ca²⁺ in SH-SY5Y cells expressing EV-A71 FLAG-2B-mCherry was determined by fluorescent assay. The SH-

SY5Y cell monolayers grew on glass slide were transfected with pLVX-puro::*FLAG-2B-mCherry* and stained apoptosis markers by FITC annexin V apoptosis detection kit I and cytoplasmic Ca²⁺ by Fluo-4 AM as described above. Controls were mCherry-transfected SH-SY5Y cells and mock transfection as described above. Images were acquired on a Zeiss LSM 800 confocal microscopy (Division of Molecular Medicine, Siriraj, Mahidol University).

Statistical analysis

Unless otherwise mentioned, all data in this study were derived from three independent experiments in triplicate samples and expressed in mean ± SE. The data from cell proliferation and viability assay, annexin V binding assay, and cytosolic Ca²⁺ detection were analyzed by using the *t* test method. The data from qRT-PCR of the apoptosis gene expression experiment was analyzed by one-way ANOVA using the SPSS 16.0 program. *P* values of <0.05 were taken to indicate statistical significance.

Results

EV-A71 2B was an enteroviral viroporin

The sequence of the cloned EV-A71 2B was composed of 294 nucleotides and 98 deduced amino acids. It shared the high nucleotide and the amino acid sequence identities, 98.5% (98% to 99%) and 96.43% (94.90% to 97.99%), respectively, with the EV-A71 2B sequences in the GenBank database. It also shared the high protein sequence identity; 92.5% (89.80% to 95.92%), with the 2B sequence of coxsackieviruses such as coxsackievirus A (CAV) 2, CAV-6, CAV-10, and CAV-16. The deduced amino acid sequence of the 2B contained putative conserved domains of 2B protein commonly found in picornaviruses designated as Pico_P2B superfamily. By comparing to the well-annotated 2B proteins from poliovirus 1 (PV-1) and coxsackievirus B3 (CVB-3), the cloned EV-A71 2B sequence was predicted to carry two hydrophobic regions called HR1 and HR2 connected by a hydrophilic spacer (Fig. 1a). The sequences of the hydrophilic spacers of EV-A71 (amino acid residues 50 to 53; DYDM), PV-1 (amino acid residues 56 to 60; RNYED) and CVB-3 (amino acid residues 58 to 62; RNHDD) were different. The HR1 exhibited an amphipathic α-helix characteristic, whereas HR2 were a completely hydrophobic helix (Fig. 1b). HR1 of EV-A71 2B contained a hydrophobic backbone and a hydrophilic face consisting of three cationic residues, one lysine (K⁺) at position 7 and two arginines (R⁺) at positions 3 and 17. A hydrophilic face on HR1 of PV-1 and CVB-3 2B contained three cationic residues of lysine (K⁺) at positions 5, 8, and 12 and

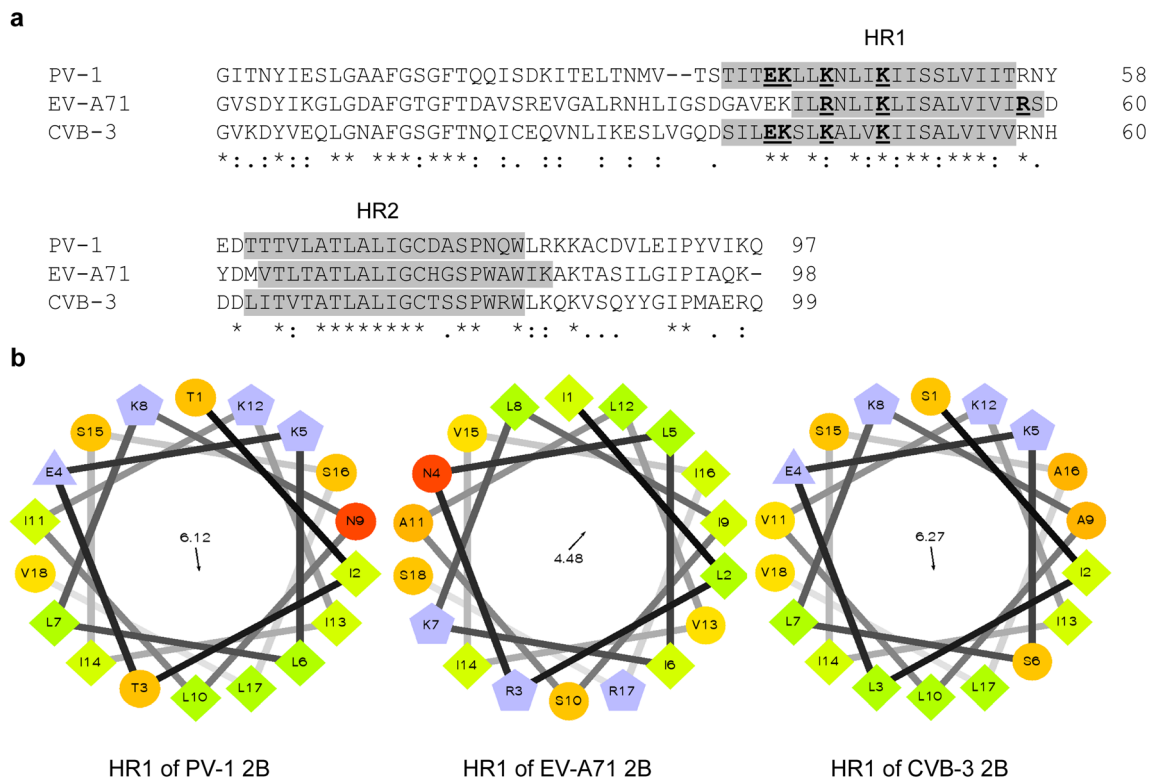


Fig. 1 EV-A71 2B had a conserved structure of enteroviral viroporin. Multiple alignment and domain predictions of CBV-3, PV-1, and EV-A71 nonstructural 2B protein sequences were demonstrated (a). The gray-shaded areas indicated the predicted HR1 and HR2 transmembrane regions of 2B sequences of EV-A71, PV-1, and CVB-3. The amino acid sequences between HR1 and HR2 were the hydrophilic spacer. Bold and underlined amino acids in the HR1 region were cationic/anionic residues located at hydrophilic face. Diagram of amphipathic α -helix wheel

depicted a top view of the amphipathic α -helix of HR1 of 2B proteins of EV-A71, PV-1, and CBV-3 (b). A hydrophilic face of EV-A71 HR1 had three cationic residues (R3, K7, and R17) and differed from PV-1 and CVB-3 which had three cationic residues (K5, K8, and K12) and one anionic residue (E4). Hydrophilic-, hydrophobic-, anionic-, and cationic residues represented by circles, diamonds, triangles, and pentagons, respectively

one anionic glutamic acid (E^-) at position 4. It was assumed that the EV-A71 2B coding sequence inserted in pLVX-puro::FLAG-2B-mCherry had complete domains of enteroviral viroporin.

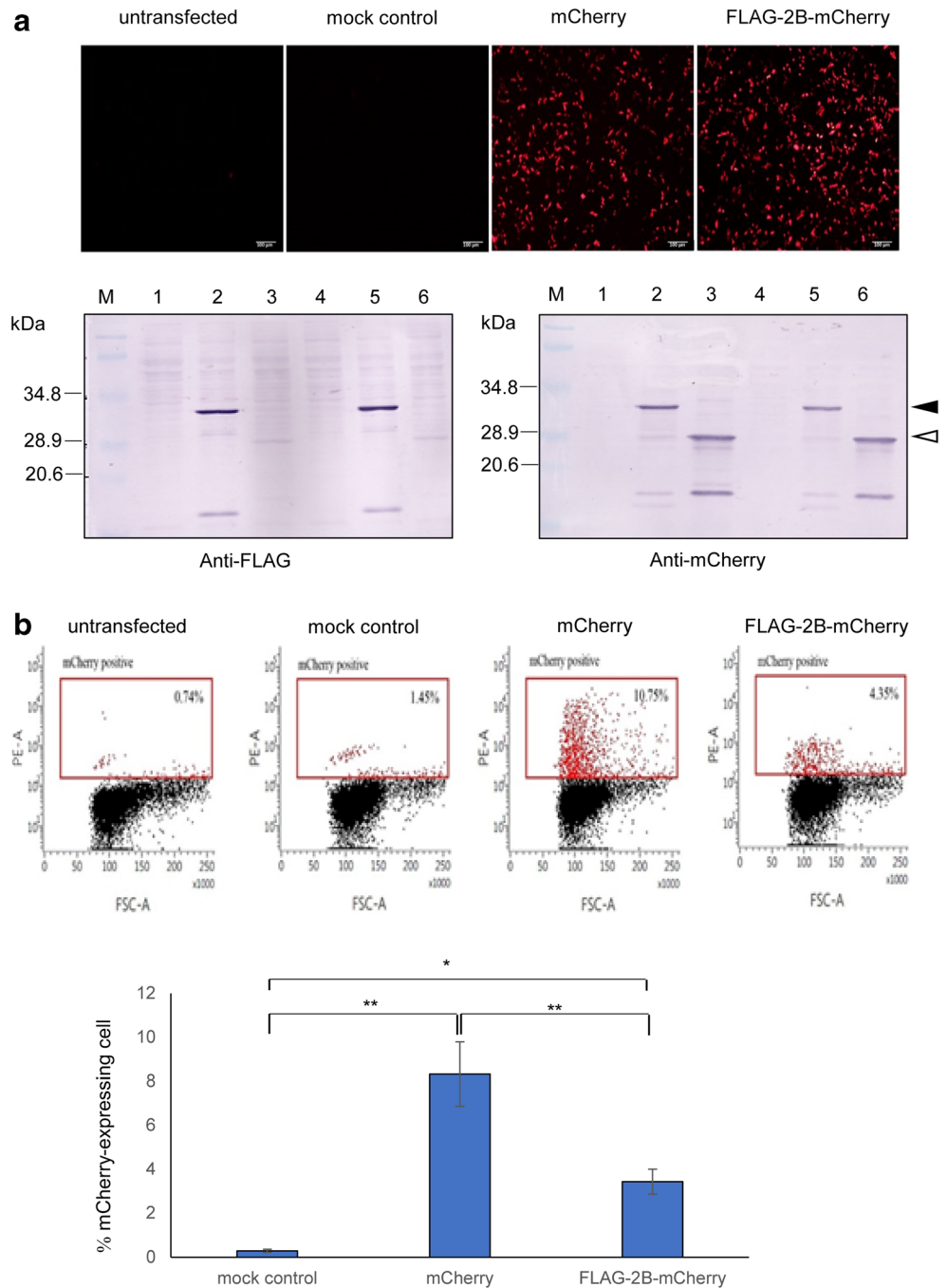
FLAG-2B-mCherry protein could be expressed in the human neuroblastoma cells

FLAG-2B-mCherry was highly expressed after transfection of HEK 293T cells for 24 h with the pLVX-puro::FLAG-2B-mCherry as shown by fluorescent microscopy and Western blotting using anti-FLAG antibody (Fig. 2a). The expression level of FLAG-2B-mCherry was similar to mCherry. The fusion of EV-A71 2B with mCherry was validated by Western blotting using anti-mCherry antibody. The FLAG-2B-mCherry was successfully expressed in the SH-SY5Y cells but the expression was lower than those of mCherry as determined by flow cytometry (Fig. 2b). It was found that $3.43 \pm 0.57\%$ and $8.3 \pm 1.5\%$ of the transfected SH-SY5Y cells expressed FLAG-2B-mCherry and mCherry, respectively. It could be concluded that the SH-SY5Y cells transiently expressed EV-A71 2B protein were successfully established.

FLAG-2B-mCherry inhibited cell growth and induced apoptosis in human neuroblastoma cells

At 24 h p.t., the cell growth was significantly higher inhibited in the SH-SY5Y transfected with pLVX-puro::FLAG-2B-mCherry than the transfected plasmids expressing FLAG-3A-mCherry and mCherry alone (Fig. 3a). The pLVX-puro::FLAG-3A-mCherry encoding EV-A71 nonstructural 3A protein which fused with FLAG-epitope tag and mCherry and expressed by the similar plasmid backbone to the FLAG-2B-mCherry. EV-A71 3A possesses different activity from EV-A71 2B, hence, the FLAG-3A-mCherry served as unrelated protein control to assure the specific activity of the 2B (Yuan et al. 2018). The percentages of the cell growth inhibition of FLAG-2B-mCherry-transfected cell were $6.67\% \pm 1.50$. SH-SY5Y cells transfected with FLAG-3A-mCherry, mCherry, and mock control did not show cell growth inhibition. The FLAG-2B-mCherry transfected cells had $6.07\% \pm 1.15$ apoptosis which was significantly higher than that of mCherry transfected- and mock cells which were $4.54\% \pm 0.75$ and $1.79\% \pm 0.29$, respectively (Fig. 3b). The SH-SY5Y infected with 0.1 and 1.0 M.O.I. of EV-A71 at

Fig. 2 FLAG-2B-mCherry was expressed in HEK 293T cells (a) and SH-SY5Y cells (b) transfected with pLVX-puro::FLAG-2B-mCherry at 24 h p.t. Red fluorescent signals of mCherry protein were detected from the human HEK 293T cells transfected with FLAG-2B-mCherry and mCherry (top, a). The FLAG-2B-mCherry fusion protein was detected by Western blotting (bottom, a) using anti-FLAG (left) and anti-mCherry (right) antibodies are indicated by the closed arrowhead. Reactive bands of mCherry protein were detected only by anti-mCherry as indicated by the opened arrowhead. Lanes 2 and 5 were homogenates and lysates from FLAG-2B-mCherry transfected cells, respectively. Lanes 3 and 6 were homogenates and lysates from mCherry transfected cells, respectively. Lanes 1 and 4 were cell fractions prepared from the mock controls. The numbers of the SH-SY5Y cells expressing FLAG-2B-mCherry and mCherry protein were quantified by flow cytometry using phycoerythrin (PE) gate (top, b). The percentages of the protein-expressing cells among SH-SY5Y cells transfected with FLAG-2B-mCherry, mCherry, and mock control subtracted with background signals from untransfected cells were compared (bottom, b). Statistical analysis was done using ANOVA *t* test and the data were expressed by mean \pm SE from three independent measurements. The levels of statistically significant differences at $p < 0.05$ and $p < 0.001$ are indicated by * and **, respectively



24 h showed $5.47\% \pm 1.55$ and $9.33\% \pm 1.58$ cell growth inhibition, respectively (Fig. 3c). The infections also induced significantly higher % apoptotic cells in the infected SH-SY5Y than the uninfected cells (Fig. 3d). The % apoptosis of the infected cells at M.O.I. of 0.1 and 1.0 were $4.42\% \pm 1.25$ and $6.80\% \pm 3.10$, respectively. The uninfected cells had $2.13\% \pm 0.90$ apoptosis. Localization of annexin V-FITC with SH-SY5Y expressing FLAG-2B-mCherry was further confirmed by confocal imaging (Fig. 4). It could be concluded that transfection of FLAG-2B-mCherry inhibited cell growth

and induced apoptosis in the SH-SY5Y cells similar to the EV-A71 infection.

CASP9 and CASP12 were upregulated in the FLAG-2B-mCherry transfected human neuroblastoma cells

The expression levels of apoptosis-related genes including CASP9 and CASP12 were significantly increased in the FLAG-2B-mCherry transfected SH-SY5Y cells at 3 and

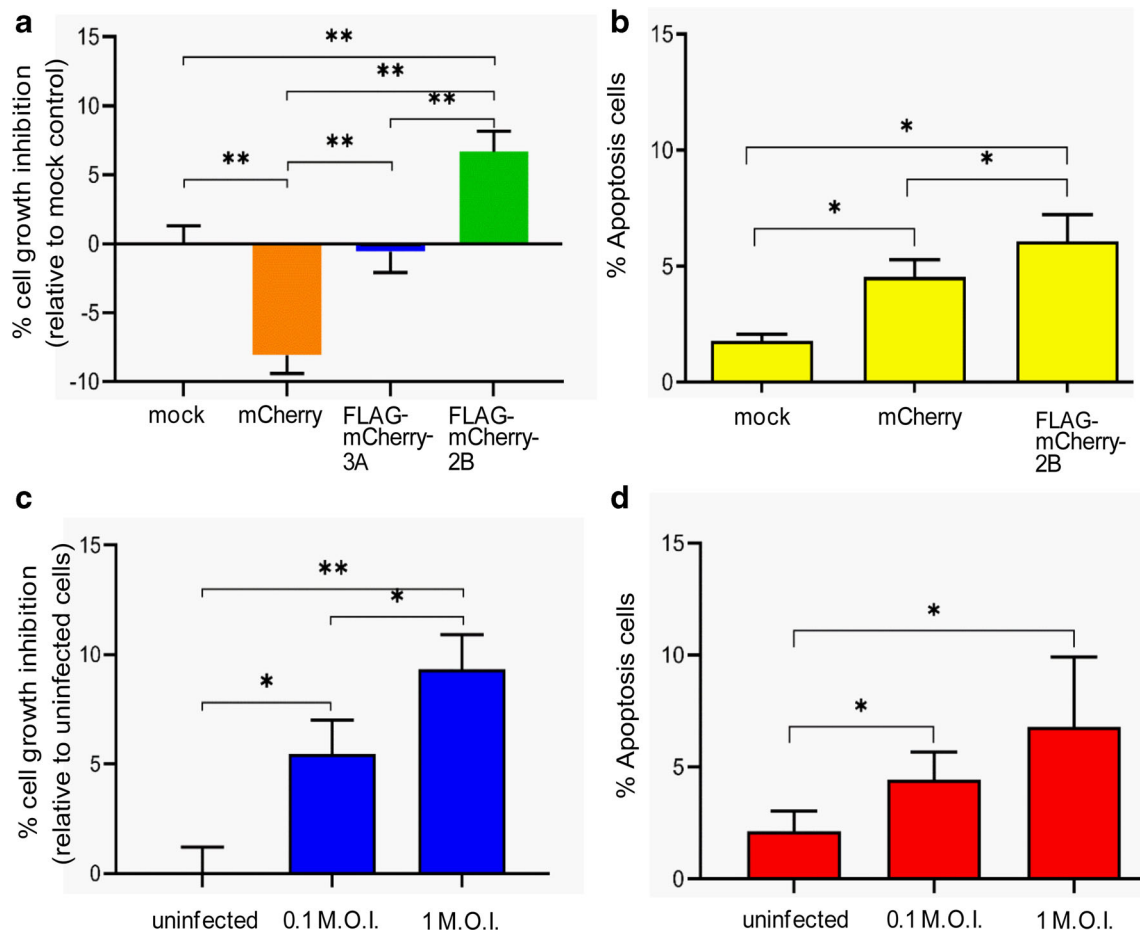


Fig. 3 FLAG-2B-mCherry inhibited the growth of SH-SY5Y (a) and induced apoptosis (b) at 24 h p.t. as determined by SRB assay and annexin V binding assay, respectively. FLAG-3A-mCherry and mCherry did not suppress proliferation of SH-SY5Y. At 24 h post-

infection, EV-A71 inhibited the growth of SH-SY5Y (c) and induced apoptosis (d) in a dose-dependent manner. The levels of statistically significant differences at $p < 0.05$ and $p < 0.001$ are indicated by * and **, respectively

24 h p.t., respectively (Fig. 5a), whereas the other selected genes did not show any significant alteration in the expression level. In the SH-SY5Y cells infected with EV-A71 at 0.1 M.O.I., it was found that the expression levels of *CASP3*, *CASP9*, and *CASP12* genes were up-regulated (Fig. 5b). The expression level of *CASP9* was significantly increased at 3 h post-infection which was higher than the other time-points. *CASP12* and *CASP3* were significantly upregulated at 12- and 24-h post-infection, respectively. *CASP8* could be amplified from RD but not SH-SY5Y (data not shown). It could be concluded that EV-A71 2B protein and the infection triggered caspase-9 and -12 in the human neuroblastoma SH-SY5Y cells.

FLAG-2B-mCherry increased cytosolic Ca^{2+} in human neuroblastoma cells

The level of cytosolic Ca^{2+} was significantly higher in the SH-SY5Y cells transfected with FLAG-2B-mCherry than the mCherry-transfected cells and the mock control at time-points

6 and 12 h p.t. and there were no significant differences for the mCherry-transfected cells compared to the mock control (Fig. 6). The concentrations of cytosolic Ca^{2+} in the FLAG-2B-mCherry-transfected SH-SY5Y cells at 1, 3, 6, 12, and 24 h p.t. were 254.40 ± 9.87 nM, 380 ± 116.30 nM, 256 ± 51.40 nM, 162 ± 8.9 nM, and 88 ± 6.62 nM, respectively. The concentrations of cytosolic Ca^{2+} in the mCherry-transfected SH-SY5Y cells at 1, 3, 6, 12, and 24 h p.t. were 195.4 ± 18.02 nM, 279 ± 31.02 nM, 114.6 ± 14.71 nM, 78.02 ± 10.55 nM, and 68.74 ± 8.32 nM, respectively. Localization of cytosolic Ca^{2+} with SH-SY5Y cells expressing FLAG-2B-mCherry was visualized by confocal imaging (Fig. 7). It was demonstrated that EV-A71 2B protein triggered the elevation of cytosolic Ca^{2+} in the human neuroblastoma SH-SY5Y cells.

Discussion

A complex interplay between the host cells and the virus determines the fate of them. The invading viruses can be sensed

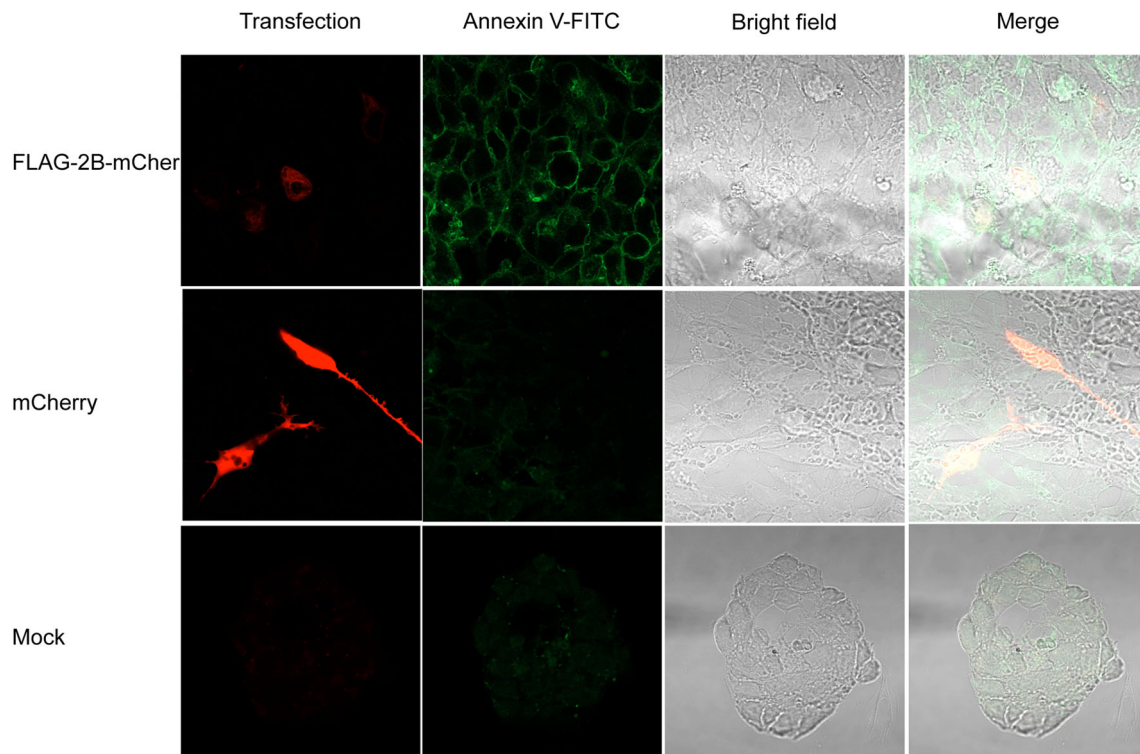


Fig. 4 At 24 h p.t., strong fluorescent densities of annexin V-FITC were visible in SH-SY5Y cells transfected with FLAG-2B-mCherry (top panels), while the signals could barely be detected in mCherry-transfected cells (middle panel) and mock control (bottom panels).

Localization of annexin V-FITC with SH-SY5Y expressing FLAG-2B-mCherry was visualized by merging the fluorescent signals and overlaying with bright field images of the cell monolayer

by the host extracellular and intracellular pathogen-related receptors (PRRs) such as Toll-like receptors and NOD-like receptors to activate the innate immune responses. The induction of early cell death is a part of the host innate defenses for shutting down the virus replication cycle by limiting the virus production. This ultimately prevents spreading of the virions into nearby cells (Roulston et al. 1999). The dying cells will expose the intracellular pathogen for clearing by the immune cells devoid of the inflammation. Consequently, the adaptive immune responses can be activated. Moreover, the viruses consume the host's resources and disturb the host cellular metabolism during the viral replication. These result in an imbalance of the cell homeostasis leading to an apoptosis induction. However, some viruses could oppose the defense system by creating a variety of strategies to modulate the apoptotic regulatory system. EV-A71 infection was found to suppress the host cell apoptosis in an early phase of the infection and promote apoptosis in the late stage (Zhang et al. 2014). It has been proposed that the anti-apoptosis state of the infecting host cells mediated by the infection is for promoting the viral progeny production by preventing a premature abortive virus replication. While the pro-apoptosis induction by the EV-A71 infection is for facilitating the virus egress and spread to infect the nearby cells. It has been proposed that dysregulation of the apoptosis mediated by the virus infection could result in aberrant cell death (Fujii et al. 2013; Lin et al.

2003; Yu et al. 2014). The massive aberrant apoptosis of the nonrenewable neurons may result in the premature loss of the cells leading to neuropathology. Nevertheless, the details mechanisms have not been elucidated.

There were several pieces of evidence showing the apoptosis-inducing activity of the EV-A71 nonstructural proteins including 2A, 2B, and 3C. The EV-A71 2A protease cleaved caspase-9 and eIF4GI resulting in an induction of apoptosis in HeLa cells (Kuo et al. 2002). EV-A71 3C protease triggers an apoptosis in the human glioblastoma SF268 cells via the mitochondrial pathway (Li et al. 2002). The EV-A71 2B protein has been demonstrated for association with the caspase-dependent apoptosis in HeLa cells (Cong et al. 2016). This evidence demonstrated that EV-A71 2B localized on the mitochondrial membrane and could directly affect the membrane potential. The altered mitochondrial membrane potential caused cytochrome c release and triggered the apoptosis. However, the apoptosis-inducing activity of EV-A71 2B and the details of the apoptosis mechanism in the neuronal cells have not been elucidated yet.

In this study, we demonstrated the apoptosis-inducing activity of EV-A71 nonstructural 2B protein in the human neuroblastoma SH-SY5Y cells. EV-A71 infection also caused SH-SY5Y cell death by inducing apoptosis. We also showed that EV-A71 3A nonstructural protein did not induce cell death in SH-SY5Y cells. Moreover, it was found that the

Fig. 5 Expression levels of the genes *CASP9* (at 3 h p.t.) and *CASP12* (at 24 h p.t.) were upregulated in the SH-SY5Y cells transfected with FLAG-2BmCherry in relative to the mCherry-transfected cells as determined by qRT-PCR (**a**). EV-A71 infection (at 0.1 M.O.I.) increased gene expression of *CASP9* (at 3 h p.t.), *CASP12* (at 12 h p.t.), and *CASP3* (at 24 h p.t.) in relative to the uninfected cells (**b**). The other selected apoptosis-related genes including *AIFM1*, *CAPN2*, and *BAX* did not alter in both transfected and infected cells. The time-point at 0 h was defined as the virus adsorption for 1 h and the RNA was immediately harvested. The levels of statistically significant differences at $p < 0.05$ and $p < 0.001$ are indicated by * and **, respectively

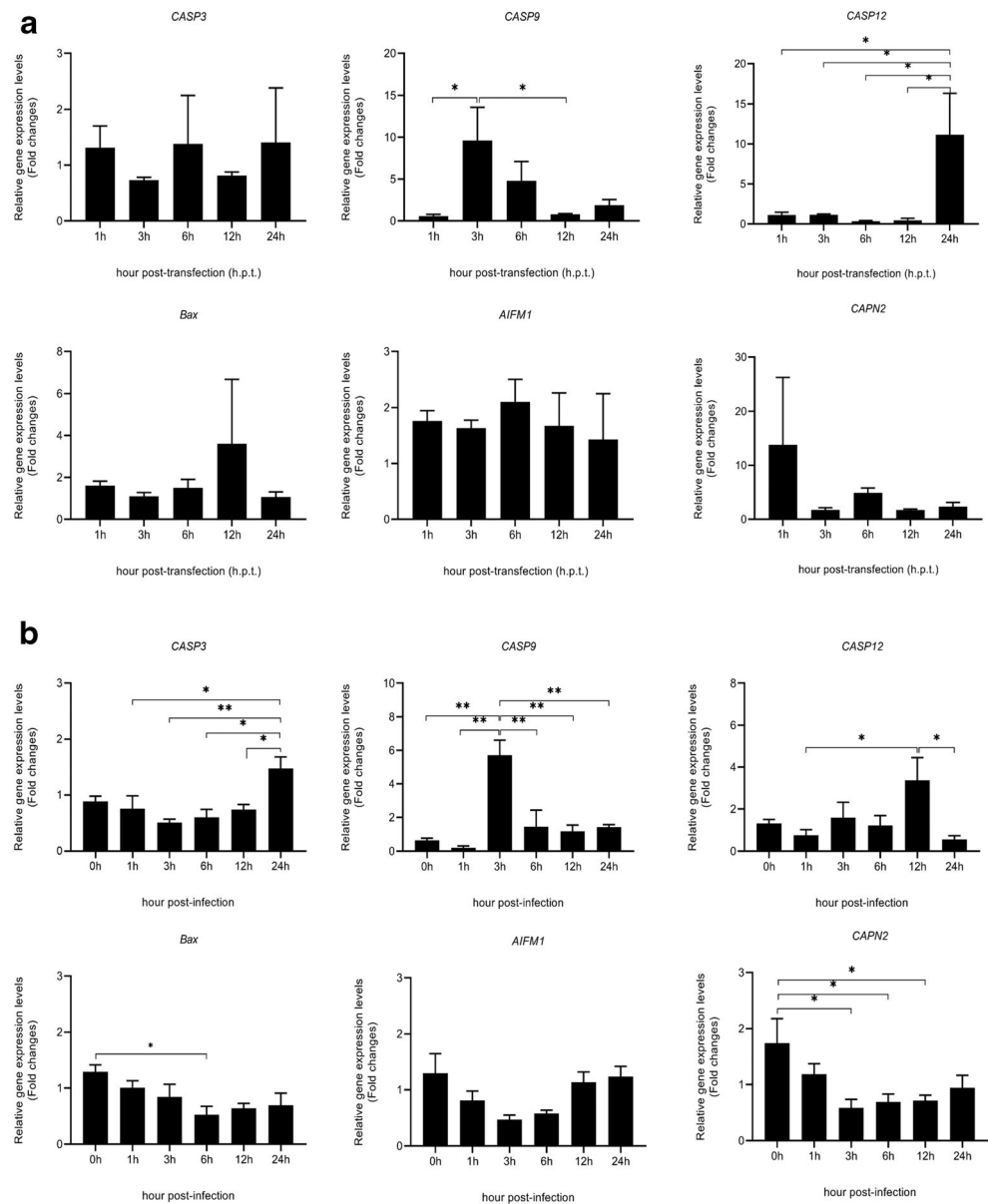
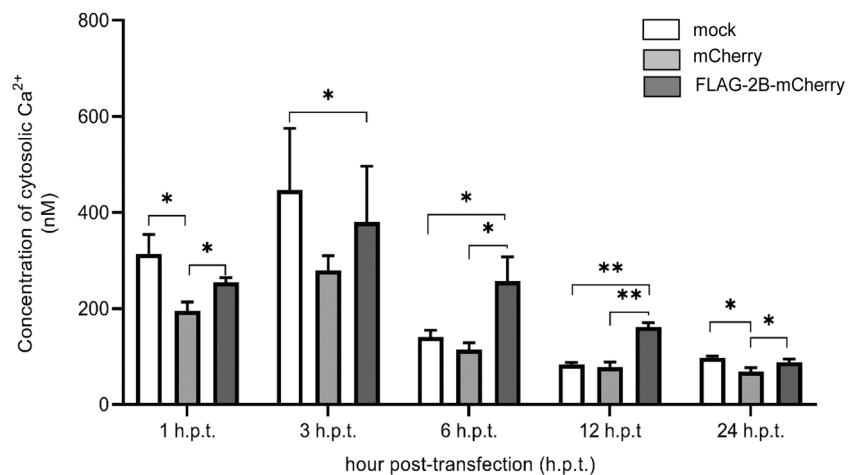


Fig. 6 Concentrations of the cytosolic calcium ion (Ca^{2+}) in FLAG-2B-mCherry transfected SH-SY5Y cells were increased at 6- and 12 h p.t. comparing to mCherry transfected cells and mock control. The levels of statistically significant differences at $p < 0.05$ and $p < 0.001$ are indicated by * and **, respectively



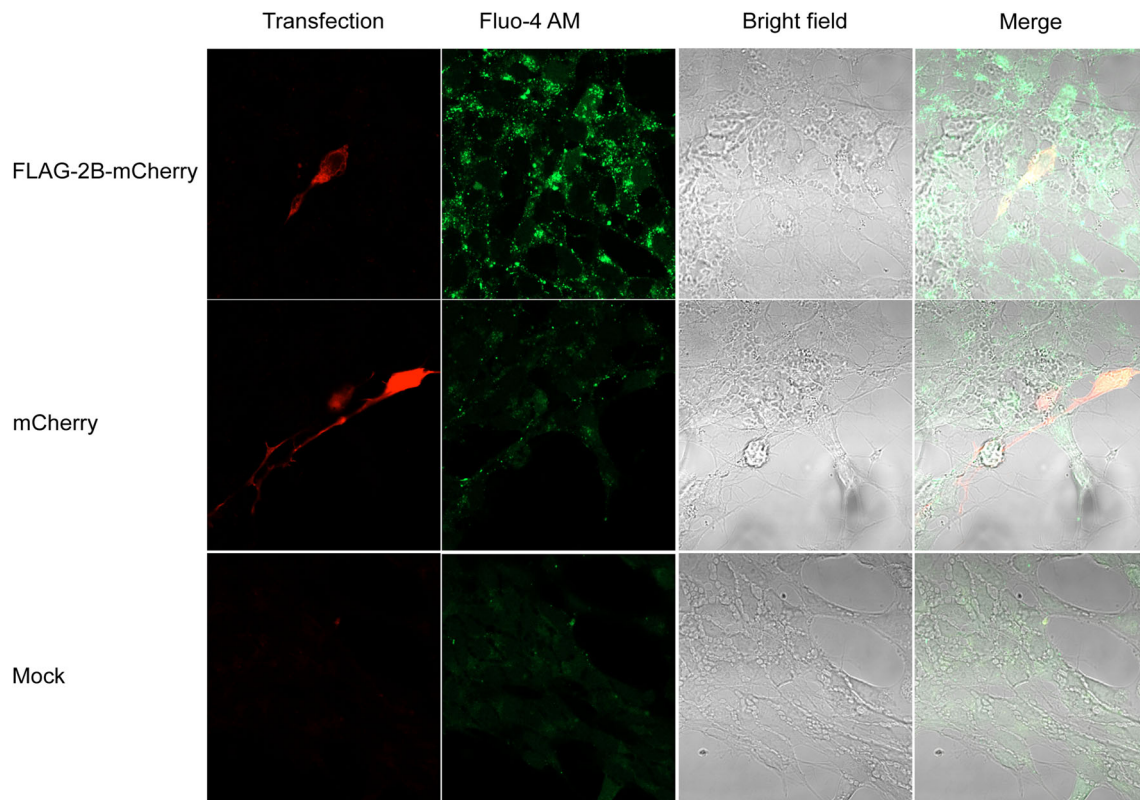


Fig. 7 At 6 h p.t., fluorescent densities of Fluo-4 AM were strongly visible in SH-SY5Y cells transfected with FLAG-2B-mCherry (top panels), while the signals could barely be detected in mCherry-transfected cells (middle panel) and mock control (bottom panels).

Localization of Fluo-4 AM with SH-SY5Y expressing FLAG-2B-mCherry was visualized by merging the fluorescent signals and overlaying with bright field images of the cell monolayer

FLAG-2B-mCherry were not colocalized with mitochondria (data not shown) which contrast to that of HeLa cells (Cong et al. 2016). It was found that the expression levels of the initiator caspase genes of the intrinsic pathway including *CASP9* and *CASP12* were up-regulated in both EV-A71 2B transfected- and EV-A71 infected SH-SY5Y cells. The pattern of dynamic changes in the gene expressions of *CASP9* and *CASP12* were also similar by which the *CASP9* came first (at 3 h p.t. in both) followed by *CASP12* (at 24 h p.t. in the 2B-transfected cells and at 12 h p.t. in the infected cells). Expression of *BAX* gene, the regulator of the intrinsic pathway, was not affected in the transfected and infected cells. The expression of *BAX* might be affected at the post-translational level. The activation of apoptosis executioner *CASP3* was detected in the infected cells but not in 2B-transfected SH-SY5Y cells. It might be attributable to the low yield of % transfection resulting in the activation of caspase-3 which was under the limit of the detection by qRT-PCR. It was found that the activation of caspase-8 was unable to be detected in SH-SY5Y cells as previously described (Cui et al. 2012). Interestingly, gene expressions of the activators of the caspase-independent pathway including *AIFM1* and *CAPN2* were not altered in both EV-A71 2B-transfected and infected SH-SY5Y cells. EV-A71 2B could trigger the elevation of

cytosolic Ca^{2+} at 6 and 12 h.p.t. which preceded the activation of *CASP12*. The EV-A71 2B sequence had the conserved structure of enteroviral viroporin similar to PV-1 and CVB-3 (de Jong et al. 2008; van Kuppeveld et al. 2005). Therefore, the increase of cytosolic Ca^{2+} in the EV-A71 2B transfected SH-SY5Y cells might be involved with conductance channel activity of the enteroviral viroporin (Scott and Griffin 2015). It could be postulated that EV-A71 2B protein mediated the caspase-dependent, intrinsic apoptosis pathway in human neuroblastoma SH-SY5Y by activating caspase-9 and -12 which associated with Ca^{2+} signaling pathway.

Recently, calcium ion (Ca^{2+}) has been reported as a second messenger coordinating ER-mitochondria interaction that triggers an apoptosis (Pinton et al. 2008). Alterations in the finely tuned intracellular Ca^{2+} homeostasis and compartmentalization in ER and mitochondria can lead to apoptosis or necrosis. ER-stress can be generated by failure in folding, sorting, and modifying the newly synthesized protein or Ca^{2+} depletion as well as alterations in the Ca^{2+} transport system in the ER. The stimuli can activate procaspase-12 by calpain and a complex of serine/threonine-protein kinase/endoribonuclease inositol-requiring enzyme 1 α (Ire1 α) and TNF receptor-associated factor-2 (TRAF-2) (Zhivotovsky and Orrenius 2011). Moreover, the

stimuli trigger efflux of Ca^{2+} restored in the ER pass through the transporter, e.g. inositol triphosphate receptor (IP3R), to the mitochondria. The released Ca^{2+} is absorbed by the mitochondria leading to a disruption of mitochondrial permeability resulting in the release of proapoptotic molecules such as cytochrome c into the cytoplasm. The released cytochrome c activates procaspase-9 through apoptosome. Together, the intrinsic pathway of apoptosis is initiated.

By the data from this study, it was proposed that EV-A71 2B protein triggered transient increased cytosolic Ca^{2+} level and associated with ER-mitochondrial interaction that activated caspase-9 and caspase-12 to drive caspase-dependent intrinsic apoptosis pathways. The mitochondrial pathway was activated earlier than the ER pathway. The detailed mechanisms warrant further studies for understanding the implication of EV-A71 infection in neuropathogenesis. The gained knowledge is essential for the development of an effective therapeutic and antiviral drug for the treatment and prevention of neurological complications caused by EV71 infection.

Authors' contributions OS conducted the overall study and data analysis; PT supervised OS on flow cytometry experiments and conducted the data analysis; PS designed the experiments and conducted the data analysis; PR constructed the recombinant plasmids; JT conceived and designed the experiments, analyzed the data, wrote a research proposal for funding and the manuscript.

Funding information This work was financially supported by the 2018–2019 fiscal year budget of the office of the National Research Council of Thailand to Thammasat University. PR received the Thammasat University Ph.D. scholarship.

Compliance with ethical standards

Consent for publication All authors consent to publication.

Conflict of interest All authors declare no personal or professional conflicts of interest, and no financial support from the companies that produce and/or distribute the drugs, devices, or materials described in this report.

Ethics approval and informed consent This article does not contain any studies with human participants performed by any of the authors.

References

- Aldabe R, Irurzun A, Carrasco L (1997) Poliovirus protein 2BC increases cytosolic free calcium concentrations. *J Virol* 71:6214–6217
- Ao D, Sun SQ, Guo HC (2014) Topology and biological function of enterovirus non-structural protein 2B as a member of the viroporin family. *Vet Res* 45:87
- Campanella M, de Jong AS, Lanke KW, Melchers WJ, Willems PH, Pinton P, Rizzuto R, van Kuppeveld FJ (2004) The coxsackievirus 2B protein suppresses apoptotic host cell responses by manipulating intracellular Ca^{2+} homeostasis. *J Biol Chem* 279:18440–18450
- Chang LY, Huang YC, Lin TY (1998) Fulminant neurogenic pulmonary oedema with hand, foot, and mouth disease. *Lancet* 352:367–368
- Chang SC, Lin JY, Lo LY, Li ML, Shih SR (2004) Diverse apoptotic pathways in enterovirus 71-infected cells. *J Neuro-Oncol* 10:338–349
- Chen CS, Yao YC, Lin SC, Lee YP, Wang YF, Wang JR, Liu CC, Lei HY, Yu CK (2007) Retrograde axonal transport: a major transmission route of enterovirus 71 in mice. *J Virol* 81:8996–9003
- Cong H, Du N, Yang Y, Song L, Zhang W, Tien P (2016) Enterovirus 71 2B induces cell apoptosis by directly inducing the conformational activation of the proapoptotic protein Bax. *J Virol* 90:9862–9877
- Cui WY, Wang J, Wei J, Cao J, Chang SL, Gu J, Li MD (2012) Modulation of innate immune-related pathways in nicotine-treated SH-SY5Y cells. *Amino Acids* 43:1157–1169
- de Jong AS, de Mattia F, van Dommelen MM, Lanke K, Melchers WJ, Willems PH, van Kuppeveld FJ (2008) Functional analysis of picornavirus 2B proteins: effects on calcium homeostasis and intracellular protein trafficking. *J Virol* 82:3782–3790
- Du X, Wang H, Xu F, Huang Y, Liu Z, Liu T (2015) Enterovirus 71 induces apoptosis of SH-SY5Y human neuroblastoma cells through stimulation of endogenous microRNA let-7b expression. *Mol Med Rep* 12:953–959
- Fujii K, Nagata N, Sato Y, Ong KC, Wong KT, Yamayoshi S, Shimanuki M, Shitara H, Taya C, Koike S (2013) Transgenic mouse model for the study of enterovirus 71 neuropathogenesis. *Proc Natl Acad Sci* 110:14753–14758
- He Y, Ong KC, Gao Z, Zhao X, Anderson VM, McNutt MA, Wong KT, Lu M (2014) Tonsillar crypt epithelium is an important extra-central nervous system site for viral replication in EV71 encephalomyelitis. *Am J Pathol* 184:714–720
- Huang CC, Liu CC, Chang YC, Chen CY, Wang ST, Yeh TF (1999) Neurologic complications in children with enterovirus 71 infection. *N Engl J Med* 341:936–942
- Huang T, Xiao Y, Yi L, Li L, Wang M, Tian C, Ma H, He K, Wang Y, Han B, Ye X, Li X (2017) Coptisine from *Rhizoma Coptidis* suppresses HCT-116 cells-related tumor growth *in vitro* and *in vivo*. *Sci Rep* 7:38524
- Kuo RL, Kung SH, Hsu YY, Liu WT (2002) Infection with enterovirus 71 or expression of its 2A protease induces apoptotic cell death. *J Gen Virol* 83:1367–1376
- Li ML, Hsu TA, Chen TC, Chang SC, Lee JC, Chen CC, Stollar V, Shih SR (2002) The 3C protease activity of enterovirus 71 induces human neural cell apoptosis. *Virology* 293:386–395
- Lin TY, Hsia SH, Huang YC, Wu CT, Chang LY (2003) Proinflammatory cytokine reactions in enterovirus 71 infections of the central nervous system. *Clin Infect Dis* 36:269–274
- Lock TJ, Parker I, Smith FI (2015) A comparison of fluorescent Ca^{2+} indicators for imaging local Ca^{2+} signals in culture cells. *Cell Calcium* 58:638–648
- Lu JR, Lu WW, Lai JZ, Tsai FL, Wu SH, Lin CW, Kung SH (2013) Calcium flux and calpain-mediated activation of the apoptosis-inducing factor contribute to enterovirus 71-induced apoptosis. *J Gen Virol* 94:1477–1485
- Martínez-Gil L, Bañó-Polo M, Redondo N, Sánchez-Martínez S, Nieva JL, Carrasco L, Mingarro I (2011) Membrane integration of poliovirus 2B viroporin. *J Virol* 85:11315–11324
- Ong KC, Badmanathan M, Devi S, Leong KL, Cardoso MJ, Wong KT (2008) Pathologic characterization of a murine model of human enterovirus 71 encephalomyelitis. *J Neuropathol Exp Neurol* 67:532–542
- Orellana EA, Kasinski AL (2016) Sulforhodamine B (SRB) assay in cell culture to investigate cell proliferation. *Bio Protoc* 6:e1984
- Pinton P, Giorgi C, Siviero R, Zecchini E, Rizzuto R (2008) Calcium and apoptosis: ER-mitochondria Ca^{2+} transfer in the control of apoptosis. *Oncogene* 27:6407–6418
- Rao X, Huang X, Zhou Z, Lin X (2013) An improvement of $2^{(-\Delta\Delta\text{CT})}$ method for quantitative real-time polymerase chain reaction data analysis. *Biostat Bioinforma Biomath* 3:71–85

- Roulston A, Marcellus RC, Branton PE (1999) Viruses and apoptosis. *Annu Rev Microbiol* 53:577–628
- Scott C, Griffin S (2015) Viroporins: structure, function and potential as antiviral targets. *J Gen Virol* 96:2000–2027
- Solomon T, Lewthwaite P, Perera D, Cardoso MJ, McMinn P, Ooi MH (2010) Virology, epidemiology, pathogenesis, and control of enterovirus 71. *Lancet Infect Dis* 10:778–790
- Srisuwan S, Tongtawe P, Srimanote P, Voravuthikunchai SP (2014) Rhodomyrtone modulates innate immune responses of THP-1 monocytes to assist in clearing methicillin-resistant *Staphylococcus aureus*. *PLoS One* 9:e110321
- Thanongsaksrikul J, Srimanote P, Tongtawe P, Glab-Ampai K, Malik AA, Supasorn O, Chiawwit P, Poovorawan Y, Chaicumpa W (2018) Identification and production of mouse scFv to specific epitope of enterovirus-71 virion protein-2 (VP2). *Arch Virol* 163:1141–1152
- Too IH, Yeo H, Sessions OM, Yan B, Libau EA, Howe JL, Lim ZQ, Suku-Maran S, Ong WY, Chua KB, Wong BS, Chow VT, Alonso S (2016) Enterovirus 71 infection of motor neuron-like NSC-34 cells undergoes a non-lytic exit pathway. *Sci Rep* 6:36983
- van Kuppeveld FJ, Galama JM, Zoll J, van den Hurk PJ, Melchers WJ (1996) Coxsackie B3 virus protein 2B contains cationic amphipathic helix that is required for viral RNA replication. *J Virol* 70:3876–3886
- van Kuppeveld FJ, de Jong AS, Melchers WJ, Willems PH (2005) Enterovirus protein 2B po(u)res out the calcium: a viral strategy to survive? *Trends Microbiol* 13:41–44
- Vichai V, Kirtikara K (2006) Sulforhodamine B colorimetric assay for cytotoxicity screening. *Nat Protoc* 1:1112–1116
- Wang C, Zhou R, Zhang Z, Jin Y, Cardona CJ, Xing Z (2015) Intrinsic apoptosis and proinflammatory cytokines regulated in human astrocytes infected with enterovirus 71. *J Gen Virol* 96:3010–3022
- Wu JM, Wang JN, Tsai YC, Liu CC, Huang CC, Chen YJ, Yeh TF (2002) Cardiopulmonary manifestations of fulminant enterovirus 71 infection. *Pediatrics* 109:E26
- Xie GC, Guo NJ, Grénman R, Wang H, Wang Y, Vuorenmaa M, Zhang Q, Zhang S, Li HY, Pang LL, Li DD, Jin M, Sun XM, Kong XY, Duan ZJ (2016) Susceptibility of human tonsillar epithelial cells to enterovirus 71 with normal cytokine response. *Virology* 494:108–118
- Yu P, Gao Z, Zong Y, Bao L, Xu L, Deng W, Li F, Lv Q, Gao Z, Xu Y, Yao Y, Qin C (2014) Histopathological features and distribution of EV-A71 antigens and SCARB2 in human fatal cases and a mouse model of enterovirus 71 infection. *Virus Res* 189:121–132
- Yuan J, Shen L, Wu J, Zou X, Gu J, Chen J, Mao L (2018) Enterovirus A71 proteins: structure and function. *Front Microbiol* 9:286
- Zhang H, Li F, Pan Z, Wu Z, Wang Y, Cui Y (2014) Activation of PI3K/Akt pathway limits JNK-mediated apoptosis during EV71 infection. *Virus Res* 192:74–84
- Zhivotovsky B, Orrenius S (2011) Calcium and cell death mechanisms: a perspective from the cell death community. *Cell Calcium* 50:211–221

Publisher's note Springer Nature remains neutral with regard to jurisdictional claims in published maps and institutional affiliations.